Biochimica et Biophysica Acta 1808 (2011) 2167–2177

Contents lists available at ScienceDirect

Biochimica et Biophysica Acta

journal homepage: www.elsevier.com/locate/bbamem

Conformational changes of β2-human glycoprotein I and lipid order in lipid–protein complexes

Mariana Paolorossi, Guillermo G. Montich *

Centro de Investigaciones en Química Biológica de Córdoba (CIQUIBIC, UNC–CONICET), Departamento de Química Biológica, Facultad de Ciencias Químicas, Universidad Nacional de Córdoba, Haya de la Torre y Medina Allende, Ciudad Universitaria, X5000HUA, Córdoba, Argentina

ARTICLE INFO

Article history:
Received 6 January 2011
Received in revised form 5 May 2011
Accepted 6 May 2011
Available online 12 May 2011

Keywords:
β2-Human glycoprotein I
Lipid membrane
FTIR
Protein conformation
Lipid–protein complex
Aggregation

ABSTRACT

We studied the conformation of β2-human glycoprotein (β2GPI) in solution and bound to the anionic lipids palmitoyl oleoyl phosphatidylglycerol (POPG), dimiristoyl phosphatidylglycerol (DMPG) and dipalmitoyl phosphatidylglycerol (DPPG) as a function of the temperature. We used the infrared amide I′ band to study the protein conformation, and the position of the antisymmetric stretching band of the methylene groups in the lipid hydrocarbon chains to study the lipid order. Lipid–protein complexes were studied in media of low and high ionic strengths. In solution, β2GPI displayed a conformational pre-transition in the range 47–50 °C, characterized by a shift in the band of β secondary structure, previous to the main unfolding at 64 °C. When the protein was bound to the anionic lipid membranes at 25 °C, a similar shift as in the pre-transition in solution was observed, together with an increase in the band corresponding to α-helix secondary structure. Lipid–protein complexes formed large aggregates within the temperature range 10≅60 °C. At temperatures above the protein unfolding, the complexes were disrupted to yield vesicles with bound protein. This finding indicated that the native fold was required for the formation of the lipid–protein aggregates. Cycles of heating and cooling showed hysteresis in the formation of aggregates.

1. Introduction

β2-Glycoprotein I (β2GPI), also known as apolipoprotein H, is a lipid-binding glycoprotein. β2GPI is abundantly present in plasma (0.2 mg/mL) and was described for the first time in 1961 by Schultze et al. [1]. β2GPI is a 54 kDa single-chain glycoprotein consisting of 326 amino acid residues, and it is composed of five short consensus repeat domains. Five carbohydrate chains contribute to almost 20% of the apparent molecular mass [2]. The first four domains have 60 amino acid residues and 4 cysteines each, with disulfide bridges joining the first to third and the second to fourth cysteines. The fifth domain is aberrant, having 82 amino acid and three disulfide bridges. Although it has been proved that both domains I and V exhibit lipid-binding properties, the fifth domain is especially important for phospholipid binding [3–6]. A positively charged region, with several lysines, between Cys281 and Cys288 in domain V is highly conserved and is involved in phospholipid binding [7–10]. The flexible loop Ser311–Lys317, containing Trp316, which is essential for phospholipid binding [11], is located in the middle of this charged region. β2GPI has an important function in blood coagulation, clearance of apoptotic bodies from the circulation [12], and it was identified as the cofactor or autoantigen in antiphospholipid syndrome (APS), which is related to venous and arterial thrombosis, fetal loss, and thrombocytopenia [13]. The physiological role of β2GPI is closely related to the capacity of binding to anionic molecules and interfaces [14–18]. Several studies performed with model lipid membrane were useful to understand the action mechanism of the protein at molecular level: the requirement of anionic lipids [17,18] indicates that electrostatics is a major driving force for membrane binding, non-polar interactions, related to the hydrophobic effect, which are also relevant for membrane binding of β2GPI [16,19], and it was also observed that native β2GPI binds to anionic lipid liposomes producing macroscopic aggregates that easily separate from the aqueous phase [14–16,20]. This property can be related to the capacity to aggregate platelets and red blood cells in vivo [21]. Studies with experimental lipid membrane systems also show that the binding occurs with conformational changes in the protein [7,22–24] and in the properties of the lipid membrane [25].

Besides helping to understand the physiological role of β2GPI, the studies with model lipid membrane are also relevant to the general problem of lipid–protein interactions. B2GPI is particularly interesting and provides an excellent model to study the behavior of a multi-domain protein with interactions due to both nonpolar and electrostatic interactions with the lipid membrane. In the present work we further studied the conformation of the protein and the order of lipids within a range of temperature that includes the gel-to-

Abbreviations: β2GPI, β2-human glycoprotein I; DPPG, 1-palmitoyl-2-palmitoyl-*sn*-glycero-3-phosphoglycerol; DMPG, 1-myristoyl-2-myristoyl-*sn*-glycero-3-phosphoglycerol; POPG, 1-palmitoyl-2-oleoyl-*sn*-glycero-3-phosphoglycerol; FTIR, Fourier transform infrared; FSD, Fourier self deconvolution

* Corresponding author. Tel.: +54 351 4334168; fax: +54 351 4334074.
E-mail address: gmontich@fcq.unc.edu.ar (G.G. Montich).

0005-2736/$ – see front matter © 2011 Elsevier B.V. All rights reserved.
doi:10.1016/j.bbamem.2011.05.007

liquid phase transition of lipids and the unfolding temperature of the protein, using infrared spectroscopy. These studies as a function of the temperature were performed to investigate the changes of stability in the membrane bound-protein and to understand the interactions responsible for the formation of lipid–protein aggregates. We observed spectroscopic changes in the band corresponding to β-chains and α-helix secondary structure in the lipid-bound protein. We showed that the aggregates produced by mixing the components at low temperatures were metastable, with changes in the protein conformation and in the order of lipid hydrocarbon chains after a cycle of heating and further cooling. We also showed that the simple titration of electrostatic charges is not the only interaction responsible to stabilize the aggregated lipid–protein complexes.

2. Materials and methods

2.1. Materials

Dimiristoyl phosphatidylglycerol (DMPG), dipalmitoyl phosphatidylglycerol (DPPG), and palmitoyl-oleoyl phosphatidylglycerol (POPG) were from Avanti Polar Lipids (Alabaster, AL). ^2H_2O 99.9+% was supplied by Nucleoeléctrica Argentina S.A. Central Nuclear Embalse, Div. Química y Procesos, NaCl, NaH_2PO_4 and Na_2HPO_4 were from J. T. Baker, Tris was from Sigma (St. Louis, MO), chlorhidric and perchloric acid 70% v/v were from Cicarelli Laboratorios (Argentina).

2.2. Purification of β2GPI

The protein was purified from human serum from several donors, generously donated by Banco de Sangre, Universidad Nacional de Córdoba, according to the method of Polz et al. [26]. Briefly, 2.5 mL of perchloric acid (70%, v/v) was added to 100 mL of fresh human serum at 4 °C. After stirring for 30 min, the sample was centrifuged for 20 min at 20,000×g. Then the supernatant was neutralized with saturated Na_2CO_3 and dialyzed against Tris/HCl buffer (20 mM Tris/HCl, pH 8.0, 0.03 M NaCl) for at least 36 h. The dialysis residue was applied to the HiPrep 16/10 Heparin FF column (Amersham Biosciences, Sweden) which had been equilibrated with the same buffer. The adsorbed proteins were eluted with 20 mM Tris–HCl buffer (pH 8.0), with increasing concentration of NaCl. The fraction that was eluted in a linear NaCl gradient from 0.3 to 0.4 M was dialyzed and further purified by anion-exchange chromatography in a Mono Q HR 5/5 column (Pharmacia, Sweden). The protein sample, checked by SDS/PAGE, showed one protein band at an apparent molecular mass of 50 kDa. Further assay by ELISA using a monoclonal antibody of human β2GPI (kindly donated by An-Na Chiang) and analysis of the N-terminal amino acid sequence (LANAIS-PRO, Laboratorio Nacional de Investigación y Servicios en Péptidos y Proteínas CONICET—Argentina) confirmed that the purified protein was β2GPI. After dialysis against MilliQ water, the purified β2GPI was freeze-dried and stored at −70 °C. Before use, the protein was solubilized in 10 mM phosphate-HCl buffer, pH 7, containing 0 or 0.1 M NaCl. The buffer was prepared in ^2H_2O for infrared experiments. Protein concentration was determined by absorption spectroscopy (ε_{280} 1.0 mL mg^{-1} cm^{-1} [27]).

2.3. Preparation of large unilamellar vesicles (LUVs)

Lipids of the desired composition were mixed in chloroform/methanol (3:1, v/v) and dried under a stream of nitrogen. Residual solvents were removed under high vacuum overnight. The lipid samples were resuspended with a solution of 10 mM phosphate-HCl plus 0 or 0.1 M NaCl, pH or pD 7. The buffer was prepared in ^2H_2O for infrared experiments. LUVs were prepared by freeze–thaw and extrusion through polycarbonate filters (pore diameter 100 nm) in an extrusion device from Avestin (Ottawa, Canada) [28]. The extrusion step was done at 25 °C for POPG, at 40 °C for DMPG and at 60 °C for DPPG. The method produced vesicles of 90 to 110 nm in diameter according to dynamic light scattering measurements.

2.4. FTIR spectroscopy

Spectra were recorded in a Nicolet Nexus spectrometer using a thermostated demountable cell for liquid samples with CaF_2 windows and 75 μm teflon spacers. For sample preparation, 0.25 mg of dry protein was resuspended with 20 μL of ^2H_2O phosphate buffer and incubated 24 h at room temperature to allow deuterium exchange of the amide protons. Then, it was mixed with 10 μL of LUVs solution at a final lipid to protein molar ratio of 100:1. The spectrometer was flushed with dry air to reduce water vapor distortions in the spectra. Normally, 50 scans were collected both for the background and the sample at a nominal resolution of 2 cm^{-1}. The temperature in the cell was controlled with a circulating water bath. The temperature setting in the bath was manually increased in steps of about 3 °C. The actual temperature in the sample, measured with a thermocouple inserted in the cell, increased continuously with a scan rate of 1 °C/min. The temperature increased steadily with the time, and the sample never spent more that few seconds at a given temperature. The contribution of the ^2H_2O to the amide I′ region was eliminated by subtracting the ^2H_2O phosphate buffer spectra acquired at the corresponding temperature. Fourier self deconvolution (FSD) was performed with the software provided with the spectrometer (Omnic software) using a bandwidth of 18 cm^{-1} and a line narrowing factor k = 2. Band fitting of the components to the original, not deconvolved spectrum was performed using the PeakFit software, according to the procedure described by Arrondo and Goñi [29] except that peak height, band width, and peak position of the components were allowed to vary one at a time. Several iterations were performed, usually 5 to 10, until the correlation coefficient was $r > 0.99$ and constant after three iterations. A linear baseline was defined between 1590 and 1690 cm^{-1} and the bands were normalized to unit area between these limits.

2.5. Isothermal titration calorimetry (ITC)

ITC experiments were done in a VP-ITC calorimeter (MicroCal, Inc). Normalized heat signals were calculated using the Origin software. In order to prevent the formation of air bubbles, samples were exhaustively degassed before being injected into the calorimetric cell. Experiments were carried out in 10 mM phosphate buffer, plus 0 or 0.1 M NaCl, at 75 °C. The reference cell was filled with water. Control titrations were performed with each sample preparation. In a typical experiment, ca. 5.5 mM titrant (LUVs) was injected into a cell containing 3 μM protein, with an injection size of 3 μL. An injection interval of 5 min was more than sufficient to allow for complete equilibration. All ITC data were analyzed and plotted in Origin software.

2.6. Turbidity assay

Turbidity of the samples as a function of the temperature was studied by measuring the absorbance at λ = 470 nm in a UV-2401 PC (Shimadzu) spectrometer, with a thermostated cell for liquid samples. Temperature scanning was at 1 °C/min.

2.7. Dynamic light scatter (DLS)

Particle size was measured, in a Nicomp 370 dynamic light scattering instrument (Nicomp Particle Sizing Systems, Santa Barbara, CA), equipped with a 30 mW laser (632.8-nm wavelength). The scattered light intensity detected at a 90° angle was treated using the Gaussian or multimodal Nicomp analysis, depending on the

polydispersity of the samples. The data presented correspond to the volume weighted distributions. The mean diameters informed were performed on different samples for periods of time long enough (from 30 min to 4 h) to collect statistically reliable data.

3. Results

We measured the infrared spectra of β2GPI to study the conformation of the protein in solution and bound to anionic lipid membranes as a function of the temperature. We also recorded the infrared bands corresponding to the lipid acyl chains and measured the turbidity of the samples. We produced a complete picture of the temperature dependence of the formation of lipid–protein aggregates and how they are related to protein conformation and lipid order.

The infrared amide I′ band contains information about the secondary structure of the protein [30]. The band components, corresponding to particular secondary structures, can be revealed by Fourier self deconvolution (FSD) of the normal spectra [31]. We also used the second derivative of the FSD spectra to determine the position of the component bands.

3.1. Conformations of β2GPI in solution

Fig. 1 shows the amide I′ absorption spectra, FSD of the normal spectra, second derivative of the FSD spectra, and band components at three representative temperatures. At 25 °C (Fig. 1, top panel), visual inspection of the FSD spectrum and its second derivative revealed four bands, they were assigned to different secondary structure element according to the classical work of Byler an Susi [31]: bands at 1636 and 1679 cm^{-1} were assigned to anti-parallel β structures, at 1663 cm^{-1} to turns, and at 1651 cm^{-1} to α-helix. These bands were clearly identified by the valleys in the second derivative. In agreement with the spectra obtained by Borchman et al. [22], a band at 1612 cm^{-1} was also observed. Because this band did not change position, width or intensity at higher temperatures either for the free protein in solution or bound to the lipid membrane, we believe that it is not due to secondary structure features of the protein but rather corresponded to the aromatic side chain of tyrosine residues in β2GPI [32,33]. Table 1 shows the location, band width and proportion of the band components. The proportion of components was in agreement with a protein containing mainly β secondary structure, although the amount of α-helix structure was over-estimated if we compare our results with the crystal structure [34]. Fig. 2 shows the variation of spectral parameters in the whole range of temperature. Fig. 2A shows the absorbance at 1630, 1636 and 1664 cm^{-1} of the normal, not deconvolved spectra, as a function of the temperature. These wavenumbers were selected to show the changes in the spectral shape. Absorbances at 1630 and 1636 cm^{-1} were chosen to monitor the disappearance of β structures. Absorbance at 1664 cm^{-1} was chosen to represent the spectral shift to larger wavenumbers. Because the component bands are relatively broad as compared to the whole spectrum, the absorbance of the normal spectrum at 1630 and 1636 cm^{-1} were representative of β structure regardless of subtle spectral shifts described below. A major spectral change with a midpoint at 64 °C was observed: the band corresponding to β secondary structure was decreased and the spectra were shifted to larger wavenumber. The comparison with the published [7], and our own differential scanning calorimetry (not shown) indicated that this transition corresponded to the main endothermic process in β2GPI unfolding. This transition at higher temperature occurred with a global shift of the spectra toward larger wavenumbers and loss of the band assigned to β secondary structure. β2GPI is composed of five well defined domains. It can be expected that these domains follow individual and to some extent independent folding–unfolding reactions. If the global unfolding reactions of these domains were actually independent, we must conclude that all they occurred at

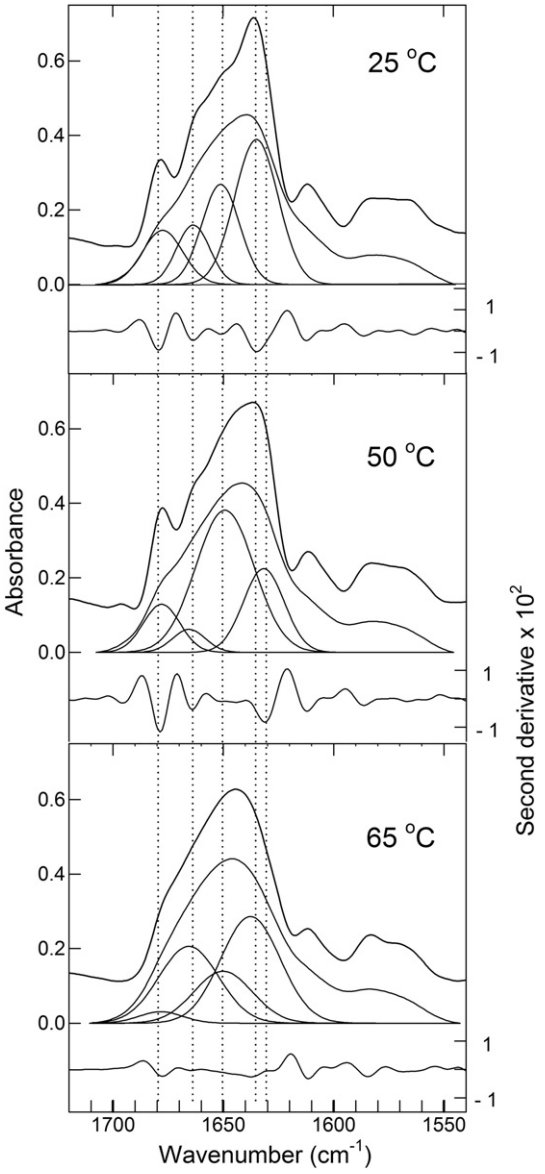

Fig. 1. Infrared absorption spectra of the amide I′ band of β2GPI at representative temperatures. For each panel the medium trace is the normal not deconvolved spectrum together with the calculated band components. Upper trace is the Fourier self deconvolved (FSD) spectrum using a factor k = 2 and a band width of 18 cm^{-1}. Lower trace is the second derivative of the FSD spectrum. Sample contained 150 μM protein, no salt added, pD = 7.4. Dotted lines are at representative wavenumbers: 1680, 1664, 1650, 1636 and 1630 cm^{-1}.

Table 1
Band components of the FTIR spectra of β2GPI at representative temperatures.

25 °C			50 °C			65 °C		
Position[a] (cm^{-1})	Width[b] (cm^{-1})	%[c]	Position[a] (cm^{-1})	Width[b] (cm^{-1})	%[c]	Position[a] (cm^{-1})	Width[b] (cm^{-1})	%[c]
1636	23	44	1631	22	24	1638	31	44
1651	20	27	1649	31	58	1650	31	22
1663	18	14	1665	17	5	1665	31	32
1679	22	15	1678	19	13	1678	23	3

Band components were fitted to the normal, not deconvolved spectra of the amide I′ absorption β2GPI in solution. Data correspond to the plots in Fig. 1.
[a] Band position after fitting procedure.
[b] Full width at the half-height.
[c] Percentage of the area of the amide band.

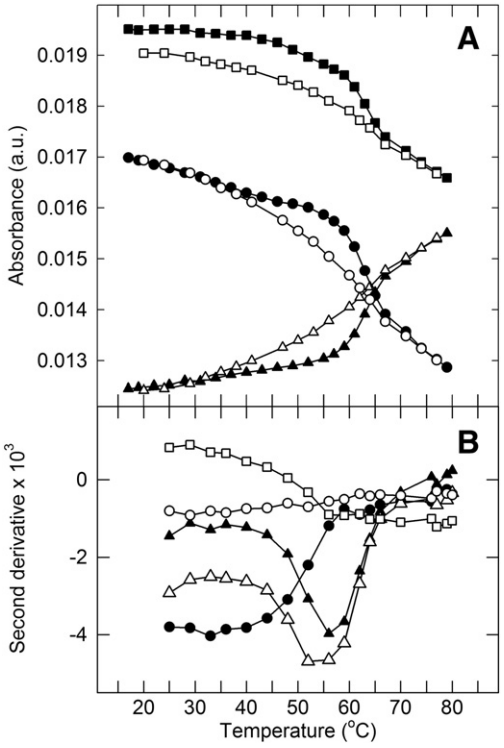

Fig. 2. Temperature dependence of the infrared spectral shape of β2GPI in solution. Panel A: absorbance of the normal, not deconvolved spectra at (●) 1630 cm^{-1} heating cycle, (○) 1630 cm^{-1} cooling cycle, (▼) 1664 cm^{-1} heating cycle, (△) 1664 cm^{-1} cooling cycle, (■) 1636 cm^{-1} heating cycle, and (□) 1636 cm^{-1} cooling cycle. Spectra were baseline subtracted and normalized to unity area between 1590 and 1690 cm^{-1}. Panel B: second derivative of the FSD spectra at (●) 1636 cm^{-1}, (▲) 1630 cm^{-1}, (△) 1678 cm^{-1}, (○) 1651 cm^{-1} and (□) 1642 cm^{-1} in the heating cycle.

about 64 °C. It must be noticed that within the experimental resolution (Fig. 2), the possible subtle differences in the temperature for the main transition in the different domains were not detected.

Subtle changes within the range 40–50 °C in the plot of absorbances at 1630 and 1636 cm^{-1} were also observed (Fig. 2A), suggesting conformational changes at a temperature below the main transition. Fig. 2B shows the values of the second derivatives of the FSD spectra at the selected wavenumbers indicated by dotted lines in Fig. 1. This procedure allowed us to detect both the major changes, already observed by inspection of the normal spectra (Fig. 2A), and the more subtle changes at lower temperature. Above 40 °C the band at 1636 cm^{-1} was shifted to lower wavenumbers: as the negative value of the second derivative measured at 1636 cm^{-1} was decreased, the value at 1630 cm^{-1} was increased. It must be noticed that this was not a continuous, monotonous change with the temperature: even when it occurred within a rather broad temperature range, the transition showed some cooperativity. The spectrum at 50 °C shown in Fig. 1, middle panel, corresponded to the conformation populated after this transition. A large proportion of β secondary structure was still present: the band at 1678 cm^{-1} and the band at lower wavenumbers, now at 1630 cm^{-1}, were still present. The band at 1651 cm^{-1} in the FSD spectra was progressively broadened yielding less clearly defined valleys in the second derivative of the FSD spectra. This transition also involved an increase in the negative value of the second derivative at 1678 cm^{-1}. At this point, we cannot differentiate if this pre-transition was due to a global change along the whole protein or circumscribed to one of the five domains. At temperatures above the main transition (Fig. 1, lower panel), the spectra showed the decrease in the band at 1630 cm^{-1} and the appearance of a band at 1638 cm^{-1}, which is close to the value of 1640 cm^{-1} assigned to unordered structure. Probably, the unfolded structures produced a band at lower wavenumber than corresponding to unordered structure because of some contribution from remaining β secondary structure that we were not able to detect.

Similar profiles as in Figs. 1 and 2 were also obtained in the presence of 0.1 M NaCl, with the difference that the transitions occurred within a slightly narrower range of temperature.

After heating above the unfolding temperature, we cooled down the samples and recorded the spectra as a function of the temperature. After the heating and cooling cycle, the global shape of the spectra was recovered. This is shown in Fig. 2 as an increase in the absorbances at 1630 and 1636, and a decrease in the absorbance at 1664 cm^{-1} in the cooling cycle (see open symbols in Fig. 2). Also, in the cooled down samples, the bands corresponding to anti-parallel structure appeared again at low temperatures. The band corresponding to β-sheet, initially at 1636 cm^{-1}, was observed after cooling, but shifted to 1630 cm^{-1}. Also the band at 1678 cm^{-1} was clearly present after cooling. Still, a relatively large proportion of unordered structure remained after cooling, as evidenced by a band at 1640 cm^{-1} (not shown). The temperature of the midpoint of the refolding transition in the cooling cycle also occurred at about 64 °C but in a less cooperative way than the unfolding (see Fig. 2). We have not detected massive aggregation of the unfolded protein at higher temperatures. Typical bands at 1616 cm^{-1} and increase in the band at 1680 cm^{-1} corresponding to aggregated unfolded structures [35] were not observed in β2GPI at high temperatures. In the absence of a bias to a massive aggregation process, an important amount of refolded structure was acquired after cooling.

Dealing with samples of β2GPI prepared from different pools of blood plasma, we observed subtle differences in the unfolding behavior. In a particular preparation, the band of β structure was already shifted to 1630 cm^{-1} at low temperature, and did not show a transition at 47 °C, although it displayed the main transition at 62 °C. These protein samples were not used in the present work; all the results shown here were done with batches displaying the behavior shown in Fig. 2.

3.2. Interaction of β2GPI with lipid membranes

Mixing β2GPI with LUVs of the anionic lipids POPG, DMPG or DPPG at low or high ionic strength produced the instantaneous formation of aggregates. After centrifugation at 13,000 × *g* in the absence of added salt or at 100,000 × *g* in samples containing 0.1 M NaCl, neither protein nor lipid was found in the supernatant. This indicated that the spectroscopic signals observed in the FTIR experiments described below, corresponded to protein–lipid complexes and contained no contribution from soluble protein or from lipids organized in structures free of protein. β2GPI remained bound to lipids within the whole range of temperature studied (see ITC experiments in Section 3.6). Similar behavior was observed in assays with lipids containing phosphatidic acid and serine in the polar head group (not shown). The global shape of the normal, not deconvolved spectra of β2GPI bound to lipid membrane was similar to the spectra of the protein in solution. After FSD, clear differences were evidenced. Fig. 3 shows the deconvolved spectra of β2GPI bound to several lipid membranes together with the second derivative of the FSD spectra. For all the studied lipids, the main features corresponding to β-sheet, the bands at 1678 and around 1630 cm^{-1}, were conserved. As already described by Borchman et al. [22] for β2GPI bound to cardiolipin, the band at 1636 cm^{-1} observed in solution, was shifted to lower wavenumbers in the anionic lipid membrane-bound protein, both in the absence of added salt or in the presence of 0.1 M NaCl. The magnitude of the shift was larger for DPPG both in the absence and in the presence of 0.1 M NaCl. Table 2 shows the position, width and proportion of the band components of β2GPI bound to the anionic

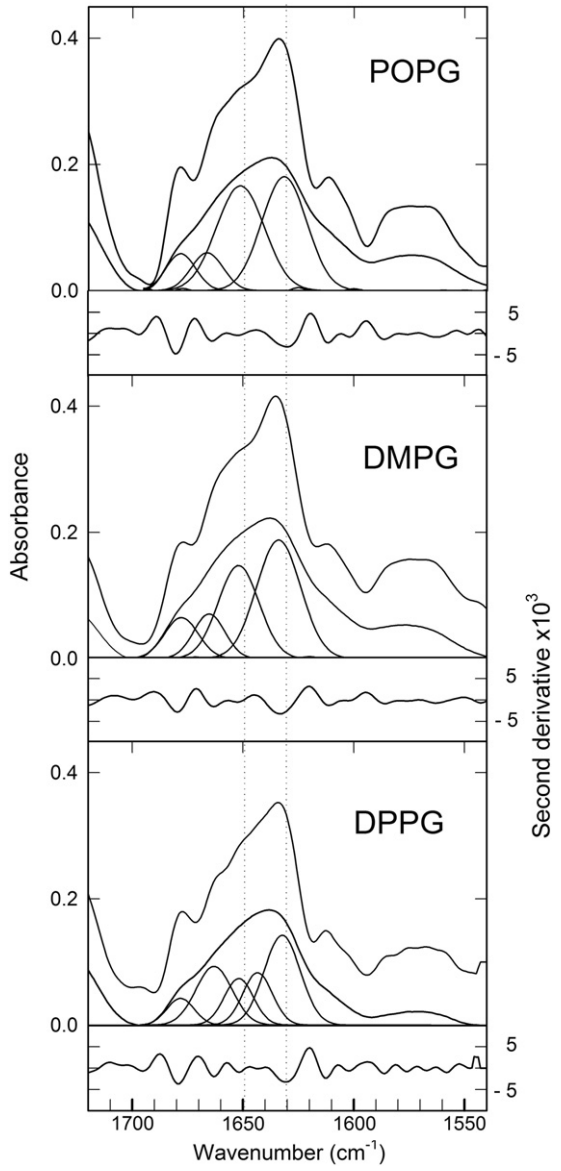

Fig. 3. Infrared absorption spectra of the amide I′ band of β2GPI in complexes with POPG, DMPG and DPPG. Traces are as in Fig. 1. Samples contained 150 μM protein, and 1.5 mM lipid. No salt added, pD = 7.4. The temperature was 23 °C. As a reference, dotted lines at 1630 and 1650 cm^{-1} were included.

lipids. For the protein bound to DMPG in 0.1 M NaCl we observed a minimal shift. Regarding the spectral shape, the major changes for the lipid-bound protein were in the central region of the spectra. Lower values for the second derivative as compared with the protein in solution were observed, indicating broader bands in the lipid-bound protein. The area of the band at 1650 cm^{-1} was increased in POPG and DMPG at low ionic strength. This result was in agreement with the increase in α-helix structure described by Wang et al. using circular dichroism [23]. For DPPG also a band at 1643 cm^{-1} corresponding to unfolded structure was observed. The increase in this band and in the band assigned to turns at 1663 cm^{-1} occurred at expenses of the bands of β structure and α-helix. Because the bands are rather wide, we cannot rule out the possible contribution of unordered structures to the area of the band at 1650/1652 cm^{-1} in POPG and DMPG. In the presence of 0.1 M NaCl, the increase in the band at 1550 cm^{-1} was smaller in POPG. In DMPG the band proportion was about the same as for the protein in solution. No

Table 2
Band components of the FTIR spectra of β2GPI in different lipid–protein complexes.

POPG				DMPG			DPPG		
Position[a] (cm^{-1})	Width[b] (cm^{-1})	%[c]		Position[a] (cm^{-1})	Width[b] (cm^{-1})	%[c]	Position[a] (cm^{-1})	Width[b] (cm^{-1})	%[c]
No salt added									
1633	22	42	*44*	1633	23	44	1631	19	36
							1643	15	17
1653	26	46	*27*	1652	21	32	1651	15	15
1667	12	3	*14*	1665	17	12	1663	19	24
1677	14	8	*15*	1677	18	12	1679	14	8
0.1 M NaCl									
1631	20	33	*44*	1634	20	43	1631	22	38
1647	23	38	*27*	1650	19	28	1651	24	40
1664	21	21	*14*	1662	17	18	1663	17	11
1679	15	8	*15*	1679	18	11	1678	16	10

Band components were fitted to the normal, not deconvolved spectra of the amide I′ absorption B2GPI. Data without added salt correspond to the plots in Fig. 3. Temperature was 23 °C. Numbers in italic in the fourth column are the values of % area for the protein in solution at 25 °C from Table 1.
[a] Band position after fitting procedure.
[b] Full with at the half-height.
[c] Percentage of the area of the amide band.

unordered structures were evidenced in DPPG, and the band assigned to α-helix was increased.

Fig. 4 shows the absorbance in the region corresponding to β structure, 1630 cm^{-1}, taken from the normal, not deconvolved spectra, as a function of the temperature for the lipid-bound protein. As for the protein in solution, we correlated the decrease of this band with the unfolding of β2GPI. We observed that the process occurred in the same cooperative way as for the protein in solution. In the absence of added salt, the temperature of the transition midpoint was lower than for the protein in solution, while in the presence of 0.1 M NaCl

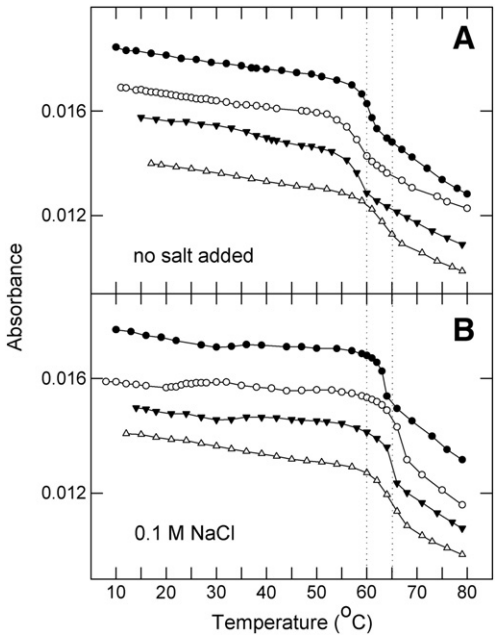

Fig. 4. Temperature dependence of the infrared spectral shape of β2GPI in lipid–protein complexes. Absorbance of the normal, not deconvolved spectra at 1630 cm^{-1}. Spectra were baseline subtracted and normalized to unity area between 1590 and 1690 cm^{-1}. Curves have an arbitrary offset for clarity. (●) POPG, (○) DMPG, (▼) DPPG, and (△) β2GPI in solution (taken from Fig. 2). Dotted lines at 60 and 70 °C are included to help recognize the shifts in the transition temperatures.

the values were equal or even slightly higher than in solution. This suggests that stronger interactions with the lipid in the absence of salt further destabilize the protein as compared with the binding in a medium with higher ionic strength. Second derivatives of the FSD spectra were not as clearly defined as for the protein in solution, mainly in the central region of the spectra. We also observed some patterns as a function of the temperature, similar to the plot in Fig. 2A, suggesting changes below the temperature for the main transition, but they were not well defined and reproducible as for the protein in solution.

3.3. The influence of membrane-bound β2GPI on the lipid acyl chain order

Infrared bands around 2920 cm^{-1} in the samples containing lipids are due to the antisymmetric stretching of C—H bonds in —CH_2— groups in the lipid acyl chains. The exact position is determined by the number of trans-gauche isomerisation and it is an index of the degree of mobility and order of the chains [36–39]. Fig. 5 shows the band position as a function of the temperature for pure POPG, DMPG and DPPG and their complexes with β2GPI. In pure DMPG and DPPG the highly cooperative transition from gel to liquid-crystalline phase was evidenced by a sharp displacement toward larger wavenumbers with midpoints of 25 and 39 °C respectively. The midpoint of the lipid phase transition was not noticeably modified although the transitions were broader in the lipid–protein complexes.

The position of the infrared band in the lipid–protein complexes was modified by β2GPI, and the effect was dependent on the ionic strength. In the absence of added salt, the binding of β2GPI produced a shift to lower wavenumbers in the studied lipids indicating an increase in the order of the hydrocarbon lipid chain. In the case of DMPG and DPPG, the shift occurred both in the gel and in the liquid crystalline phase of the lipid (see Fig. 5). In the presence of 0.1 M NaCl instead, the ordering effect of β2GPI on the lipid hydrocarbon chains was observed only above 30 °C. Below 30 °C the membrane-bound protein induced no shift in the infrared bands of POPG, DMPG and DPPG. In the lower panels of Fig. 5, it can be seen that the wavenumbers for the pure lipid were coincident with the values for the lipid with bound protein until 30 °C approximately. Few data points around 30 °C shifted from the value for the pure lipid for the complexes with DPPG, 0.1 M NaCl. Although small, the shift was reproducible and followed the trend observed at the same temperature in POPG, indicating that the ordering effect of the protein starting above 30 °C was superimposed to the changes due to the gel to liquid-crystalline phase transition in DPPG. Even when the pre-transition of the protein in solution was evidenced above 40 °C, subtle changes can already occur at 30 °C triggering the interaction with the lipid.

Thermal unfolding of β2GPI around 60 °C in the lipid–protein complexes produced two remarkable effects: the disruption of the aggregates and the decrease in the order of lipid hydrocarbon chains. Fig. 5 shows that the wavenumber of the —CH— stretching bands above 60 °C were slightly, but consistently larger in the lipid–protein complexes than in the pure lipid. The unfolding of lipid-bound protein, as detected by the changes in the amide I′ band, occurred at different temperatures within the range 58–65 °C depending on the lipid–protein complexes: in the absence of salt it was at 60 °C for POPG and 58 °C for DMPG and DPPG, in the presence of added salt it was few degrees above 60 °C. The observation that the temperature of the transition midpoint for the change in the lipid order as measured by the —CH_2— stretching followed this trend, further confirmed that it was coupled to the unfolding of β2GPI.

The shift of the lipid infrared band to lower wavenumbers always occurred with formation of large complexes. At this point, we do not know if the shift was due to a direct effect of the protein on the lipid structure or if it was a consequence of the long-range organization and lipid–lipid interactions mediated by the protein.

3.4. Formation of the lipid–protein complexes

Fig. 6 shows the turbidity of the samples, measured by the absorbance at 470 nm, as a function of the temperature. DLS of the samples was also measured at selected temperatures to evaluate the size of the aggregates. As described in Section 3.2, mixing the protein with the LUVs produced aggregates that were easily separated from the aqueous phase. In the absence of added salt these aggregates were more turbid than in the presence of 0.1 M NaCl (compare the turbidity at 20 °C in the upper with the lower panels in Fig. 6). The average

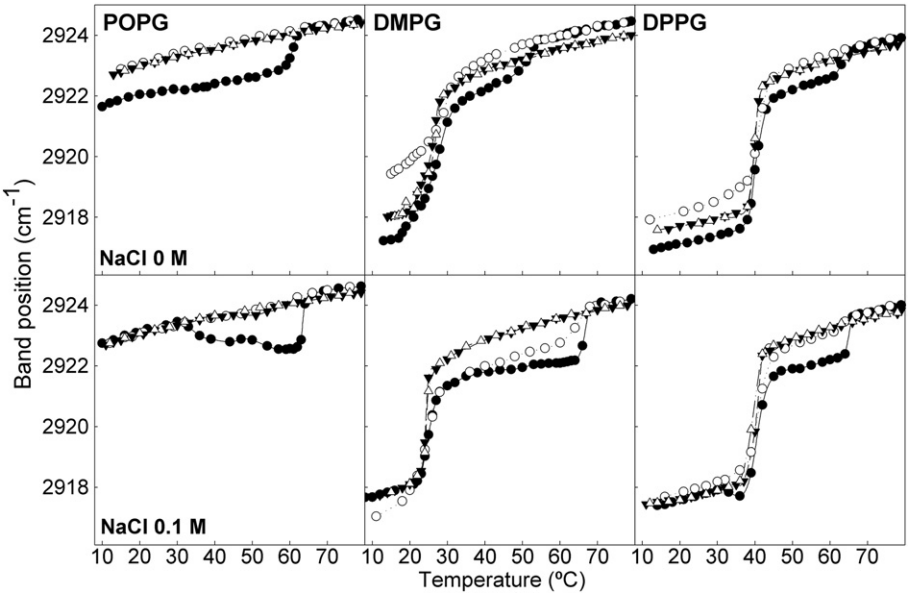

Fig. 5. Temperature dependence of the position of the antisymmetric stretching absorption band of —CH_2—. First line: no salt added. Second line: 0.1 M NaCl. Lipids are indicated in the corresponding column. (●) β2GPI + LUVs, heating cycle; (○) β2GPI + LUVs, cooling cycle; (▲) pure LUVs, heating cycle; (△) pure LUVs, cooling cycle.

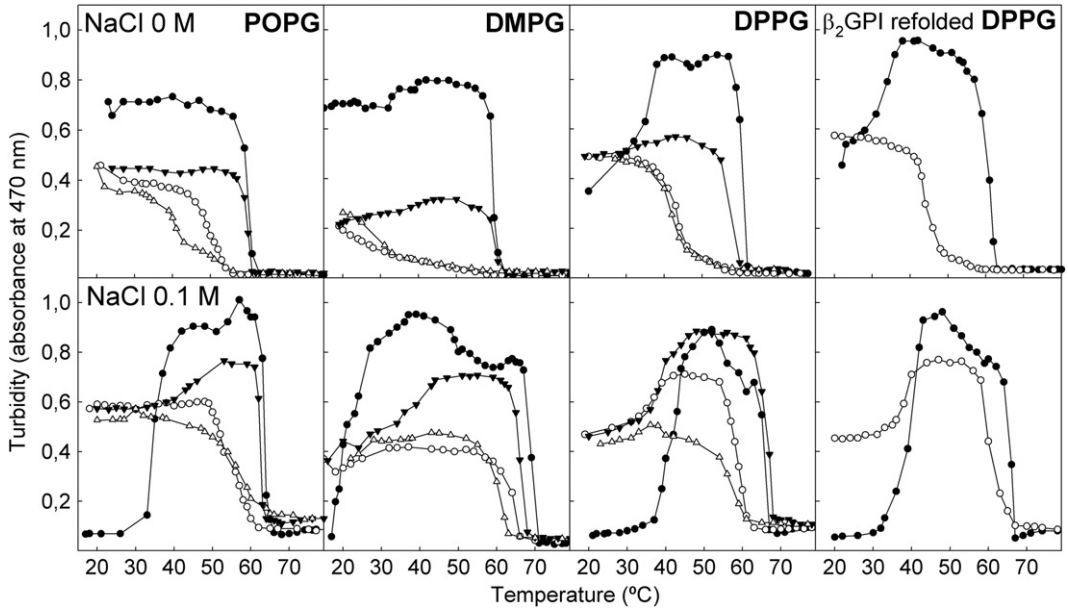

Fig. 6. Light dispersion of the complexes of β2GPI with POPG, DMPG and DPPG. First line: no salt added; second line: 0.1 M NaCl. Lipids are indicated in the corresponding column. Right column: the protein was heated to 80 °C and cooled to 10 °C in solution before mixing with the lipid.

diameter, at low ionic strength, was larger than 6000 nm and the population was wide dispersed, with a standard deviation of 1000 nm. In the samples containing 0.1 M NaCl, and below 30 °C, the aggregates were of an average diameter of 200 nm in the case of POPG and DPPG LUVs. For the complexes with DMPG, similar diameters were observed below 23 °C. The increase of turbidity as a function of the temperature was in agreement with the temperature at which changes in lipid hydrocarbon chain order started (previous section and Fig. 5) and the aggregates were also larger than 6000 nm average diameter. In all cases, the disruption of the aggregates as detected by decrease in turbidity was in agreement with the temperature for protein unfolding. DLS measurements of the disrupted aggregates at 70 °C showed structures with diameters of about 100 nm in all cases.

3.5. Hysteresis in the formation of aggregates, protein conformation and lipid order

After heating to temperatures above the protein unfolding and disruption of the aggregates, we cooled down the samples and followed the changes in the turbidity of the sample and the infrared spectroscopic changes in the protein and lipids.

Fig. 6 shows the changes of turbidity in two cooling cycles. In a first cooling cycle, POPG–, DMPG–, and DPPG–protein aggregates recovered the turbidity, but this occurred at temperatures considerably lower than in the heating cycle. This was observed whether at low or high ionic strength. In a second heating cycle, aggregates were again dissociated, according to the decrease in turbidity at about 60 °C, as in the first heating cycle. In a second cooling cycle, turbidity again increased at the same lower temperature as in the first cooling cycle.

After cooling from 70 °C, the spectra of β2GPI recovered the general features corresponding to β secondary structure. As also observed for the protein in solution, some degree of unfolded protein was obtained after cooling.

In the previous sections we described that the order of lipid hydrocarbon chains decreased when the bound protein was unfolded and the aggregates were disrupted in a first heating cycle around 60 °C. In the cooling cycle, this effect was not observed in POPG and DPPG: the cooperative changes in the lipid order occurred only at the temperature of the lipid main transition in DPPG and the lipid order was equal to the pure lipid in POPG (see Fig. 5). The same was true for DMPG in the absence of added salt, but in the presence of 0.1 M NaCl the cooling was trough a path similar to the heating cycle (Fig. 5). The degree of order reached after cooling was also dependent on the lipid and ionic strength condition. In the absence of salt, DMPG and POPG reached a more unordered state than the pure lipid.

When the protein was unfolded in solution by heating to 80 °C and then cooled down to 10 °C, it was able to produce the same effect on

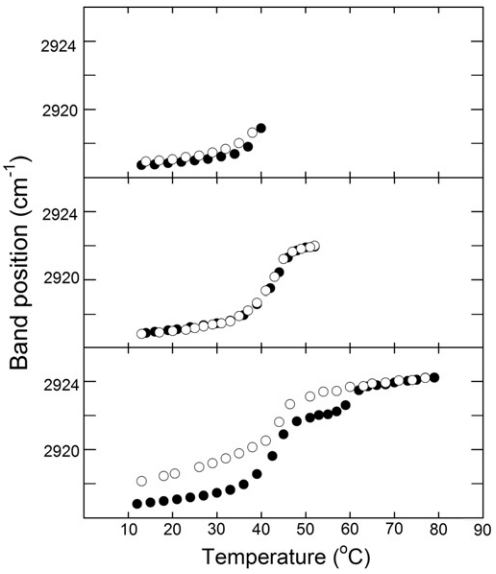

Fig. 7. Temperature dependence of the position of the antisymmetric stretching absorption band of —CH_2—. (●) Heating and (○) cooling to intermediate temperatures.

the lipid order shown in Fig. 5 for DPPG in the absence of salt, and on the formation of complexes for DPPG as shown in Fig. 6.

To investigate which was the step that leaded the complexes to a state that displayed hysteresis, we heated the complexes to different temperatures and then cooled down the sample to the initial temperature. Fig. 7 shows that only after heating above the temperature of protein unfolding, the system returned through a different path. This indicates that only after protein unfolding in the complexes, the system can explore different conformations and cross over to a state that will return to low temperatures through a different path.

3.6. Isothermal titration calorimetry

To understand the mechanism for the disruption of aggregates, and consequently, to understand the forces involved in the formation of the aggregates, it was necessary to know if the protein remained bound to the membrane above 60 °C. It was technically difficult to study the protein binding to lipid membranes by filtration or centrifugation at high temperature. ITC, instead, provided a reliable way to study the binding process at high temperatures. Fig. 8 shows the heat released when a DPPG LUVs suspension was titrated into a β2GPI solution. The exothermic process evidenced the interaction of the protein with the anionic lipid at 75 °C. We considered a simple model in which one protein binds to a cluster of 10 lipids. Choosing this cluster size was arbitrary and based on the average dimensions of the protein. The same conclusions regarding the degree of binding in the FTIR experiments (see below) were reached assuming a cluster of 20 or 5 lipids. It was shown that β2GPI does not produce a disruption of the bilayer structure and intermixing of lipids [21,25,34]. Then, we considered that the protein does not penetrate into the inner volume of liposomes and that only half of the lipid was available for protein binding. Again, assuming accessibility to the whole amount of lipids both in the ITC and in the FTIR experiments we reached the same conclusion regarding the amount of bound protein in an FTIR experiment. Suitable controls, titrating DPPG into a solution in the absence of protein or the LUVs made of dipalmitoyl phosphatidyl choline (a zwitterionic lipid to which β2GPI does not bind) into a solution containing β2GPI, showed that no heat was exchanged and we concluded that the spikes of heat exchange shown in Fig. 8 were due specifically to the binding of the protein to the anionic lipid.

By fitting the experimental data to the assumed model, we obtained binding constants $K_{0NaCl} = 2.46 \times 10^6\ M^{-1}$ in the absence of added salt and $K_{0.1NaCl} = 1.4 \times 10^5\ M^{-1}$ in 0.1 M NaCl. Using these binding constant we calculated that in the experimental conditions of the FTIR measurements 98% of the protein was bound to the lipid whether in the absence of added salt or in the presence of 0.1 M NaCl. For the experimental conditions used in the turbidity measurements in Fig. 7, the amounts were 98% bound in the absence of salt and 66% in the presence of 0.1 M NaCl. If we assume that the system reaches the same final state by mixing the components at low temperature and then increasing the temperature or by mixing the components at 75 °C, as in the ITC experiment, we can conclude that in the FTIR and turbidity experiments, β2GPI remained bound to the lipid membranes in the disaggregated complexes at high temperature in the absence of salt.

ITC experiments were mainly performed to know if β2GPI was bound to lipid membranes at high temperatures. Besides concluding that the protein was actually bound at high temperature, these experiments also yield valuable information about the nature of binding at high temperature. From the associations constants, Kas, mentioned above, we calculated the binding standard free energy as $\Delta G^0 = -RT\ln(Kas.55.5)$ where R is the gas constant, T the absolute temperature and the factor 55.5, the molar concentration of water. By multiplying by this factor, the binding constant in $molar^{-1}$ units was transformed into an adimensional binding constant expressed as a function of molar fraction of reactants and product. Standard enthalpy ΔH^0 was calculated by fitting the experimental heat uptakes in Fig. 8 to the binding model, and the contribution of entropy by $T\Delta S^0 = \Delta G^0 + \Delta H^0$. At 75 °C, in the absence of added salt we obtained $\Delta G^0_{0NaCl} = -12.9$ kcal mol^{-1}, $\Delta H^0_{0NaCl} = -48.6$ kcal mol^{-1} and $T\Delta S^0_{0NaCl} = -35.7$ kcal mol^{-1}. In the presence of 0.1 M NaCl we obtained $\Delta G^0_{0.1NaCl} = -10.98$ kcal mol^{-1}, $\Delta H^0_{0.1NaCl} = -59.66$ kcal mol^{-1} and $T\Delta S^0_{0.1NaCl} = -48.77$ kcal mol^{-1}. Clearly, the favorable free energy of binding was contributed by the enthalpic term. The binding reaction occurred against an unfavorable decrease in the entropy. This is not in agreement with the characteristics of a binding driven mainly by electrostatic interactions. Binding of charged peptides to anionic lipid membranes, for example, was

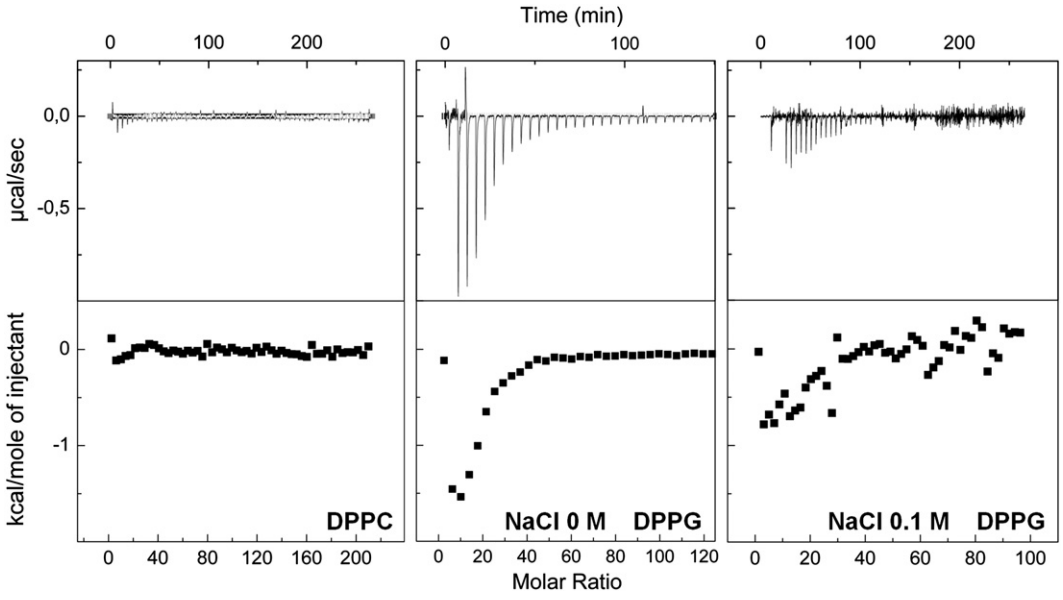

Fig. 8. Isothermal titration calorimetry of β2GPI with LUVs at 75 °C. Top line: Cp, bottom line: ΔH. Left panel: β2GPI + DPPC, NaCl 0M. Middle panel: β2GPI + DPPG, NaCl 0M. Right panel: β2GPI + DPPG, NaCl 0.1 M.

described to occur with negligible change in enthalpy and driven by an increase of entropy due water release [42]. We conclude that other driving forces different from electrostatics are important at high temperature, most probably favorable van der Waals interactions. It could be proposed that the decrease in entropy was due to the loss of degree of freedom when the flexible, unfolded protein in solution was bound to the lipid. β2GPI does not bind to zwitterionic lipids, like phosphatidylcholine, at low temperature. This was previously described [23] and our centrifugation assays (not shown) were in agreement. Then, we included a control experiment performing the titration of β2GPI with POPC vesicles (Fig. 7). No heat exchange was observed in this case. Considering that no binding was observed at low temperature using physical separations, it is probable that the absence of heat exchange was actually due to the lack of binding. Still, we have not rigorously proved that binding to zwitterionic membranes does not occur at high temperatures with $\Delta H = 0$.

4. Discussion

We studied the conformation of β2GPI and the order of hydrocarbon lipid chains as a function of the temperature. Comparing the thermal unfolding process in the membrane with the process in solution allowed us to infer about the lipid–protein interactions at physiological temperatures. We also described the thermodynamic functions driving the binding of unfolded β2GPI to lipid membranes at high temperatures. At the present, this information is not available for the native protein at lower temperatures and cannot be extrapolated from the measurements at high temperature, obviously because the folded and unfolded protein must interact differently with membranes. Besides of technical difficulties in the measurements, thermodynamic functions at physiological temperatures are difficult to be interpreted in this system because they include the energetic of both protein binding an lipid aggregation process.

We found that thermal unfolding of β2GPI is a complex process, both for the protein in solution and in lipid–protein complexes. Different states were populated as the temperature increased. In solution, a major conformational change with disappearance of the infra red bands assigned to β structures was observed at 64 °C. It was coincident with the main heat uptake in DSC experiments [7]. We detected more subtle changes at lower temperature, 47–50 °C, as a shift of the infrared band at 1636 to 1630 cm^{-1}. This shift can be due to an effective conformational change leading to different torsion angles in the amide group and changes in the distribution of the hydrogen bonds involved in the β secondary structure. It can also be due to an increase in fluctuations leading to exchange of H atoms by ^{2}H atoms from the solvent. If this was the case, the number of protected H atoms seems to be small because we did not observe major changes at the wavenumber corresponding to the amide II band, changes that would be expected if H atoms were exchanging with ^{2}H from the solvent (see for example [40]). Considering the modular structure of β2GPI, it is not surprising the occurrence of a complex unfolding. The pre transition, for example, could be easily explained if we apply the considerations presented above, to a single domain in the protein. That is, the unfolding of a single domain could produce the spectral changes observed at low temperature. What was actually surprising was the relatively large cooperativity of the transition at 60 °C. Because of the small number of contacts between domains, as compared with the intradomain contacts, it could be speculated that domains have independent folding reaction. Different temperatures for those reactions should produce spectroscopic changes spread over a wide temperature range. Observed the unfolding at a single temperature, we should conclude that if the domains are not coupled, the transition occurs at the same temperature for all of them.

A similar shift from 1636 cm^{-1} to lower wavenumbers as observed at about 40 °C in solution, was observed at 25 °C when β2GPI was bound to the anionic lipids, although the magnitude of the shift was dependent on the particular lipid. Because of the similarity in the spectral change, it could be proposed that binding to anionic lipids produced the same conformational changes as observed at 47–50 °C in solution. The binding to the lipids did not affect the global structure of the protein: all the bands observed in solution were present in the lipid-bound protein. Only in the case of DPPG at low ionic strength appeared a band for unordered structure. The picture that we present here is that binding to anionic lipids induced the formation of helix structures and also some unordered structures that cannot be clearly resolved from the band at 1650 cm^{-1}. Stronger interactions, with DPPG for example, can further induce the unfolding of some regions in the protein. The global unfolding was still cooperative and at about the same temperature as in solution. In the absence of salt, unfolding of the membrane-bound protein occurred at lower temperatures, about 5 °C, than in solution or in the presence of 0.1 M NaCl. This observation can also be framed within the modular structure of β2GPI: several authors agree in considering the fifth domain as the main responsible for membrane binding [17,18,34], but the role of the rest of the protein is also recognized, mainly for the formation of aggregates at low ionic strength. Then, it could be possible that in the presence of salt we were observing the unfolding of domains 1 to 4, exposed to aqueous medium at the same temperature as the soluble protein. In the absence of salt, domains 1 to 4 could be involved in further interactions with membranes inducing their apposition. These interactions can result in a decreased stability and lower unfolding temperature. Protein conformational changes in the lipid–protein complexes were not occurring in an inert, not reacting interface. Instead, they were coupled to changes in the order of lipid acyl chains and in the long-range organization of the lipid–protein aggregates. Binding to the anionic lipid membranes produced the aggregation of LUVs and the formation of larger complexes. Electrostatic interactions have been clearly described as driving forces for the binding of β2GPI to lipid membranes [7,19]. The dependence on the size and sedimentation properties of the aggregates with the ionic strength described here, indicated that electrostatics also determined the interactions that leaded to aggregation. We do not present here a quantitative measurement of the strength of the complex formation as a measurement of binding free energy in the whole range of temperature, but it can be considered qualitatively that the formation of aggregates was stronger in low ionic strength: the aggregates were larger, were sedimented more easily, and at high temperature the binding constant was larger in the absence of salt than in the presence of 0.1 M NaCl. Because the increase of ionic strength should operate in the opposite way and favor the aggregation of like-charged vesicles, it can be concluded that salt influences on the strength of the aggregates through its influence on the protein binding. According to the anionic lipid:protein relation that we used here, the negative charge in the vesicles was not completely titrated. Then, it is remarkable that β2GPI can still induce aggregation between charged vesicles.

The structure of the lipid–protein aggregates, regarding protein conformation and lipid order, showed a complex dependence with the temperature. Aggregates were formed at low temperatures, and the degree of perturbation induced in the order of the lipid hydrocarbon chains was dependent on the ionic strength of the solution, suggesting that the stronger the binding of the protein the larger the lipid perturbation. This difference could be originated in radically different ways of interaction depending on the salt concentration. The perturbation of the lipid order, and its dependence with ionic strength, as measured by FTIR spectroscopy was in agreement with measurements performed with fluorescent probes [25]. Clearly, increases in the strength of electrostatic interactions at low ionic strength induced more perturbation of the membrane hydrocarbon core, probably due to further penetration of the protein. It is interesting that even when the temperature for the gel to liquid

crystalline transition was not changed, the order of lipid chains was increased both in the gel and liquid crystalline phase while the system was in the aggregated form, that is below 60 °C.

Thermal unfolding of the protein produced the disassembling of the aggregates. Size measurement by DLS of the resulting structures above 60 °C showed particles of about 100 nm and ITC measurements showed that the protein was bound. It must be noticed that unfolded bound protein should still neutralize the opposite charges of lipids. Nevertheless, thermally unfolded, membrane-bound protein, was not able to support aggregation of vesicles. We conclude that the specific fold of β2GPI was required for vesicle aggregation.

After cooling from high temperatures, the hydrocarbon lipid chains in the lipid–protein complexes were more disordered than in the initial aggregates formed at low temperature. This change occurred only after protein unfolding as shown in Fig. 7, heating at temperatures close, but lower, to the unfolding temperature returned the system to at the same state. Then we conclude that the aggregates produced by mixing the components at low temperature are metastable structures. This observation is particularly interesting because it means that different kind of aggregates, regarding lipid and protein order, could be obtained at low temperature if suitable catalytic path were present. Metastability was determined by the nature of the lipid–protein complexes. It must be emphasized that hysteresis was an emerging property of the complexes. It was not due to possible hysteresis in the folding–unfolding of the protein. β2GPI has key roles in the process of platelets aggregation and generation of antiphospholipid antibodies [18,21,41]. Studies with model membrane systems have been useful to understand physical aspects of the interaction with lipids: it is known that electrostatics play an essential role in the interaction [7,16] and that hydrophobic interactions are also established with the membranes [19,24]. Increase in the lipid order and protein conformational changes were also described by measuring the fluorescence anisotropy of membrane probe [17] and protein infrared spectra [22]. Here we show that subtle differences in the protein conformational change were dependent on the nature of the anionic lipid. This observation is relevant to understand the action mechanisms of β2GPI: it means that changes in the local membrane lipid composition are candidates to participate in the control of the immunogenicity of this protein through the regulation of the exposure of different epitopes.

Acknowledgments

We are indebted to Banco de Sangre UNC, for the kind donation of human plasma, to Nucleoeléctrica Argentina S.A. Central Nuclear Embalse, Div. Química y Procesos for the kind donation of ^2H_2O and to Dr. An-Na Chiang, National Yang-Ming University, Taipei, Taiwan for kind donation of the β2GPI antibody. This work was supported with grants from CONICET, SECyT-UNC, FONCyT, and MINCyT-Córdoba. MP was recipient of a doctoral fellowship from SECyT-UNC and CONICET.

References

[1] H.E. Schultze, Glycoproteins of human plasma, Bull. Schweiz. Akad. Med. Wiss. 17 (1961) 77–91.
[2] J.N. Lozier, N. Takahashi, F.W. Putnam, Complete amino acid sequence of human plasma beta 2-glycoprotein I, Proc. Natl. Acad. Sci. U. S. A. 81 (1984) 3640–3644.
[3] Y. Hagihara, K. Enjyoji, T. Omasa, Y. Katakura, K. Suga, M. Igarashi, E. Matsuura, H. Kato, T. Yoshimura, Y. Goto, Structure and function of the recombinant fifth domain of human beta 2-glycoprotein I: effects of specific cleavage between Lys77 and Thr78, J. Biochem. 121 (1997) 128–137.
[4] Y. Hagihara, Y. Goto, H. Kato, T. Yoshimura, Role of the N- and C-terminal domains of bovine beta 2-glycoprotein I in its interaction with cardiolipin, J. Biochem. 118 (1995) 129–136.
[5] M. Hoshino, Y. Hagihara, I. Nishii, T. Yamazaki, H. Kato, Y. Goto, Identification of the phospholipid-binding site of human beta(2)-glycoprotein I domain V by heteronuclear magnetic resonance, J. Mol. Biol. 304 (2000) 927–939.
[6] D.P. Hong, Y. Hagihara, H. Kato, Y. Goto, Flexible loop of beta 2-glycoprotein I domain V specifically interacts with hydrophobic ligands, Biochemistry 27 (2001) 8092–8100.
[7] M. Hammel, R. Schwarzenbacher, A. Gries, G.M. Kostner, P. Laggner, R. Prassl, Mechanism of the interaction of beta(2)-glycoprotein I with negatively charged phospholipid membranes, Biochemistry 40 (2001) 14173–14181.
[8] A. Steinkasserer, P.N. Barlow, A.C. Willis, Z. Kertesz, I.D. Campbell, R.B. Sim, D.G. Norman, Activity, disulphide mapping and structural modelling of the fifth domain of human beta 2-glycoprotein I, FEBS Lett. 313 (1992) 193–197.
[9] J. Hunt, S. Krilis, The fifth domain of beta 2-glycoprotein I contains a phospholipid binding site (Cys281–Cys288) and a region recognized by anticardiolipin antibodies, J. Immunol. 15 (1994) 653–659.
[10] Y. Sheng, A. Sali, H. Herzog, J. Lahnstein, S.A. Krilis, Site-directed mutagenesis of recombinant human beta 2-glycoprotein I identifies a cluster of lysine residues that are critical for phospholipid binding and anti-cardiolipin antibody activity, J. Immunol. 15 (1996) 3744–3751.
[11] D.A. Horbach, E. van Oort, M.J. Tempelman, R.H. Derksen, P.G. de Groot, The prevalence of a non-phospholipid-binding form of beta2-glycoprotein I in human plasma. Consequences for the development of anti-beta2-glycoprotein I antibodies, Thromb. Haemost. 80 (1998) 791–797.
[12] T.A. Brighton, P.J. Hogg, Y.P. Dai, B.H. Murray, B.H. Chong, C.N. Chesterman, Beta 2-glycoprotein I in thrombosis: evidence for a role as a natural anticoagulant, Br. J. Haematol. 93 (1996) 185–194.
[13] M. Blank, D. Faden, A. Tincani, J. Kopolovic, I. Goldberg, B. Gilburd, F. Allegri, G. Balestrieri, G. Valesini, Y. Shoenfeld, Immunization with anticardiolipin cofactor (beta-2-glycoprotein I) induces experimental antiphospholipid syndrome in naive mice, J. Autoimmun. 7 (1994) 441–455.
[14] H. Wurm, Beta 2-Glycoprotein-I (apolipoprotein H) interactions with phospholipid vesicles, Int. J. Biochem. 16 (1984) 511–515.
[15] Z. Kertesz, B.B. Yu, A. Steinkasserer, H. Haupt, A. Benham, R.B. Sim, Characterization of binding of human beta 2-glycoprotein I to cardiolipin, Biochem. J. 15 (1995) 315–321.
[16] Y. Hagihara, D.P. Hong, M. Hoshino, K. Enjyoji, H. Kato, Y. Goto, Aggregation of beta (2)-glycoprotein I induced by sodium lauryl sulfate and lysophospholipids, Biochemistry 22 (2002) 1020–1026.
[17] S.X. Wang, G. Cai, S. Sui, Intrinsic fluorescence study of the interaction of human apolipoprotein H with phospholipid vesicles, Biochemistry 38 (1999) 9477–9484.
[18] G.M. Willems, M.P. Janssen, M.M. Pelsers, P. Comfurius, M. Galli, R.F. Zwaal, E.M. Bevers, Role of divalency in the high-affinity binding of anticardiolipin antibody-beta 2-glycoprotein I complexes to lipid membranes, Biochemistry 35 (1996) 13833–13842.
[19] S.X. Wang, G.P. Cai, S.F. Sui, The insertion of human apolipoprotein H into phospholipid membranes: a monolayer study, Biochem. J. 15 (1998) 225–232.
[20] I. Schousboe, Purification, characterization and identification of an agglutinin in human serum, Biochim. Biophys. Acta 28 (1979) 396–408.
[21] M. Lokar, J. Urbanija, M. Frank, H. Hägerstrand, B. Rozman, M. Bobrowska-Hägerstrand, A. Iglič, V. Kralj-Iglič, Agglutination of like-charged red blood cells induced by binding of β2-glycoprotein I to outer cell surface, Bioelectrochemistry 73 (2008) 110–116.
[22] D. Borchman, E.N. Harris, S.S. Pierangeli, O.P. Lamba, Interactions and molecular structure of cardiolipin and beta 2-glycoprotein 1 (beta 2-GP1), Clin. Exp. Immunol. 102 (1995) 373–378.
[23] S.-X. Wang, Y.-T. Sun, S.-F. Sui, Membrane-induced conformational change in human apolipoprotein H, Biochem. J. 348 (2000) 103–106.
[24] F. Wang, X.-F. Xia, S.-F. Sui, Human apolipoprotein H may have various orientations when attached to lipid layer, Biophys. J. 83 (2002) 985–993.
[25] A.T. Lee, K. Balasubramanian, A.J. Schroit, Beta(2)-glycoprotein I-dependent alterations in membrane properties, Biochim. Biophys. Acta 20 (2000) 475–484.
[26] E. Polz, H. Wurm, G.M. Kostner, Investigations on beta 2-glycoprotein-I in the rat: isolation from serum and demonstration in lipoprotein density fractions, Int. J. Biochem. 11 (1980) 265–270.
[27] H. Kato, K. Enjyoji, Amino acid sequence and location of the disulfide bonds in bovine beta 2 glycoprotein I: the presence of five Sushi domains, Biochemistry 30 (1991) 11687–11694.
[28] M.J. Hope, M.B. Bally, G. Webb, P.R. Cullis, Production of large unilamellar vesicles by a rapid extrusion procedure. Characterization of size distribution, trapped volume and ability to maintain a membrane potential, Biochim. Biophys. Acta 812 (1985) 55–65.
[29] J.L. Arrondo, F.M. Goñi, Structure and dynamics of membrane proteins as studied by infrared spectroscopy, Prog. Biophys. Mol. Biol. 72 (1999) 367–405.
[30] J.L. Arrondo, A. Muga, J. Castresana, F.M. Goñi, Quantitative studies of the structure of proteins in solution by Fourier-transform infrared spectroscopy, Prog. Biophys. Mol. Biol. 59 (1993) 23–56.
[31] D.M. Byler, H. Susi, Examination of the secondary structure of proteins by deconvolved FTIR spectra, Biopolymers 25 (1986) 469–487.
[32] A. Barth, The infrared absorption of amino acid side chains, Prog. Biophys. Mol. Biol. 74 (2000) 141–173.
[33] K.D. Sharma, L.A. Andersson, T.M. Loehr, J. Terner, H.M. Goff, Comparative spectral analysis of mammalian, fungal, and bacterial catalases. Resonance Raman evidence for iron-tyrosinate coordination, J. Biol. Chem. 264 (1989) 12772–12779.
[34] B. Bouma, P.G. de Groot, J.M. van den Elsen, R.B. Ravelli, A. Schouten, M.J. Simmelink, R.H. Derksen, J. Kroon, P. Gros, Adhesion mechanism of human beta (2)-glycoprotein I to phospholipids based on its crystal structure, EMBO J. 18 (1999) 5166–5174.

[35] W.K. Surewicz, J.J. Leddy, H.H. Mantsch, Structure, stability, and receptor interaction of cholera toxin as studied by Fourier-transform infrared spectroscopy, Biochemistry 29 (1990) 8106–8111.
[36] D.G. Cameron, H.L. Casal, H.H. Mantsch, Y. Boulanger, I.C. Smith, The thermotropic behavior of dipalmitoyl phosphatidylcholine bilayers. A Fourier transform infrared study of specifically labeled lipids, Biophys. J. 35 (1981) 1–16.
[37] D. Carrier, M. Pézolet, Raman spectroscopic study of the interaction of poly-L-lysine with dipalmitoylphosphatidylglycerol bilayers, Biophys. J. 46 (1984) 497–506.
[38] L.K. Tamm, S.A. Tatulian, Infrared spectroscopy of proteins and peptides in lipid bilayers, Q. Rev. Biophys. 30 (1997) 365–429.
[39] K. Cieślik-Boczula, A. Koll, The effect of 3-pentadecylphenol on DPPC bilayers ATR-IR and 31P NMR studies, Biophys. Chem. 140 (2009) 51–56.
[40] H.H. de Jongh, E. Goormaghtigh, J.-M. Ruysschaert, Amide-proton exchange of water-soluble proteins of different structural classes studied at the submolecular level by infrared spectroscopy, Biochemistry 36 (1997) 13603–13610.
[41] J. Urbanija, N. Tomsic, M. Lokar, A. Ambrozic, S. Cucnik, B. Rozman, M. Kanduser, A. Iglic, V. Kralj-Iglic, Coalescence of phospholipid membranes as a possible origin of anticoagulant effect of serum proteins, Chem. Phys. Lipids 150 (2007) 49–57.
[42] G. Montich, S. Scarlata, S. McLaughlin, R. Lehrmann, J. Seelig, Thermodynamic characterization of the association of small basic peptides with membranes containing acidic lipids, Biochim. Biophys. Acta 1464 (1993) 17–24.